Available online at www.sciencedirect.com

ScienceDirect

Solar Energy 110 (2014) 561–577

SOLAR ENERGY

www.elsevier.com/locate/solener

Direct normal irradiance related definitions and applications: The circumsolar issue

P. Blanc [a,*], B. Espinar [a], N. Geuder [b], C. Gueymard [c], R. Meyer [d], R. Pitz-Paal [e], B. Reinhardt [f,g], D. Renné [h], M. Sengupta [i], L. Wald [a], S. Wilbert [j]

[a] *MINES ParisTech, PSL Research University, O.I.E. – Centre Observation, Impacts, Energie, CS 10207, rue Claude Daunesse, 06904 Sophia Antipolis Cedex, France*

[b] *Stuttgart University of Applied Sciences, Schellingstrasse 24, 70174 Stuttgart, Germany*

[c] *Solar Consulting Services, P.O. Box 392, Colebrook, NH 03576, USA*

[d] *Suntrace GmbH, Brandstwiete 46, 20457 Hamburg, Germany*

[e] *DLR, Institute of Solar Research, Linder Höhe, 51170 Cologne, Germany*

[f] *DLR, Institute for Atmospheric Physics, Oberpfaffenhofen, Germany*

[g] *Meteorologisches Institut, Ludwig-Maximilians-Universität, Munich, Germany*

[h] *National Renewable Energy Laboratory (Emeritus), 15013 Denver West Parkway, Golden, CO 80401, USA*

[i] *National Renewable Energy Laboratory, 15013 Denver West Parkway, Golden, CO 80401, USA*

[j] *DLR, Institute of Solar Research, Plataforma Solar de Almeria (PSA), Ctra. de Senés s/n km 4, Apartado 39, 04200 Tabernas, Spain*

Received 6 June 2014; received in revised form 12 September 2014; accepted 2 October 2014
Available online 21 October 2014

Communicated by: Associate Editor Frank Vignola

Abstract

The direct irradiance received on a plane normal to the sun, called direct normal irradiance (DNI), is of particular relevance to concentrated solar technologies, including concentrating solar thermal plants and concentrated photovoltaic systems. Following various standards from the International Organization for Standardization (ISO), the DNI definition is related to the irradiance from a small solid angle of the sky, centered on the position of the sun. Half-angle apertures of pyrheliometers measuring DNI have varied over time, up to ≈10°. The current recommendation of the World Meteorological Organization (WMO) for this half-angle is 2.5°. Solar concentrating collectors have an angular acceptance function that can be significantly narrower, especially for technologies with high concentration ratios. The disagreement between the various interpretations of DNI, from the theoretical definition used in atmospheric physics and radiative transfer modeling to practical definitions corresponding to specific measurements or conversion technologies is significant, especially in the presence of cirrus clouds or large concentration of aerosols. Under such sky conditions, the circumsolar radiation—*i.e.* the diffuse radiation coming from the vicinity of the sun—contributes significantly to the DNI ground measurement, although some concentrating collectors cannot utilize the bulk of it. These issues have been identified in the EU-funded projects MACC-II (Monitoring Atmospheric Composition and Climate-Interim Implementation) and SFERA (Solar Facilities for the European Research Area), and have been discussed within a panel of international experts in the framework of the Solar Heating and Cooling (SHC) program of the International Energy Agency's (IEA's) Task 46 "*Solar Resource Assessment and Forecasting*". In accordance with these discussions, the terms of reference related to DNI are specified here. The important role of circumsolar radiation is evidenced, and its potential contribution is evaluated for typical atmospheric conditions. For thorough analysis of performance of concentrating solar

* Corresponding author at: MINES ParisTech, Centre Observation, Impacts, Energie (O.I.E.), CS 10207, rue Claude Daunesse, F-06904 Sophia Antipolis Cedex, France. Tel.: +33 (0)4 93 95 74 04; fax: +33 (0)4 93 67 89 08.
E-mail address: philippe.blanc@mines-paristech.fr (P. Blanc).

http://dx.doi.org/10.1016/j.solener.2014.10.001
0038-092X/

systems, it is recommended that, in addition to the conventional DNI related to 2.5° half-angle of today's pyrheliometers, solar resource data sets also report the sunshape, the circumsolar contribution or the circumsolar ratio (CSR).

Keywords: Direct normal irradiance; Circumsolar irradiance; Circumsolar ratio; Pyrheliometer; Concentrating solar technologies

Nomenclature

ACR	active cavity radiometer
AOD	aerosol optical depth
COST	European cooperation in science and technology
CPV	concentrating photovoltaic
CSNI	circumsolar normal irradiance
CSP	concentrating solar power
CSR	circumsolar ratio
CST	concentrating solar technologies
DNI	direct normal irradiance
IEA	International Energy Agency
LBNL	Lawrence Berkeley National Laboratory
MACC	Monitoring Atmospheric Composition and Climate
MYSTIC	Monte Carlo for the physically correct tracing of photons in cloudy atmospheres
OPAC	optical properties of aerosols and clouds
PVPS	photovoltaic power systems
RSI	rotating shadowband irradiometer
SAM	solar (or system) advisor model
SFERA	Solar Facilities for the European Research Area
SHC	Solar Heating and Cooling
SMARTS	simple model of the atmospheric radiative transfer of sunshine
SOD	slant optical depth
SolarPACES	solar power and chemical energy systems
WIRE	weather intelligence for renewable energy
WMO	World Meteorological Organization
L	broadband sky radiance
θ_s	solar zenith angle
ξ	angular distance from the center of the sun
φ	azimuth angle of a given point in the sky in the orthogonal spatial system of axes defined by the direction of the sun (see Fig. 1)
B_n	broadband DNI
P	penumbra function or acceptance function
δ_s	half-angle of the sun disk
S_s	sunshape
B_n^{strict}	non-scattered direct normal irradiance (non-scattered radiant flux from the sun disk only)
E_n^{toa}	extraterrestrial normal irradiance of the sun
α	opening half-angle
Ω	viewing angle
θ_c	acceptance half-angle
C	concentration factor
α_s	slope angle
α_l	limit angle
B_n^{ideal}	ideal DNI
B_n^{sun}	DNI of the sun (radiant flux from the sun disk only)
CS_n	CSNI
CS_n^{ideal}	ideal CSNI
CSR	circumsolar ratio
CSC	circumsolar contribution
τ	aerosol optical depth
η	Ångström exponent
d_{550}	slant aerosol optical depth at 550 nm

1. Introduction

The direct irradiance received on a plane normal to the sun over the total solar spectrum is defined as direct normal irradiance (DNI). DNI is an essential component of global irradiance, especially under cloudless conditions, and represents the solar resource that can be used by various forms of concentrating solar technologies (CST), such as concentrating solar power (CSP) systems—also called solar thermal electricity systems, including parabolic dish, parabolic trough, linear-Fresnel, or solar tower, or concentrating photovoltaic (CPV) systems.

For that reason, the characterization of the solar resource in terms of quantities related to DNI is of particular importance, and presently corresponds to one of the primary research topics in the domains of solar radiation modeling, satellite-based retrievals, and radiometric ground-based measurements. In the fields of electromagnetic scattering, radiative transfer and atmospheric optics, many decades of theoretical developments in so-called "directional radiometry" are noteworthy, as recently reviewed by Mishchenko (2011, 2014). Such highly fundamental studies have reached the solar energy community only indirectly, however.

Despite the fact that the term "*direct normal irradiance*" and its corresponding acronym DNI have been widely used for a long time in the fields of solar energy and solar resource assessment, this quantity may actually correspond to different definitions, interpretations or usages, which can lead to confusion.

These issues have been identified in two EU-funded projects, namely MACC-II (Monitoring Atmospheric Composition and Climate-Interim Implementation) and SFERA (Solar Facilities for the European Research Area). Moreover, experts participating in the International Energy Agency Solar Heating and Cooling Programme (IEA SHC) Task 46 "*Solar Resource Assessment and Forecasting*" extensively discussed these issues at two international workshops. This collaborative IEA Task is also coordinating with both the IEA SolarPACES (solar power and chemical energy systems) and IEA PVPS (photovoltaic power systems) implementing agreements. Thus, international experts from all relevant solar technologies—most particularly CSP and CPV—have been involved to reach a consensus on these definitions.

DNI is defined as follows in the ISO-9488 standard (ISO-9488, 1999): "*Direct irradiance is the quotient of the radiant flux on a given plane receiver surface received from a small solid angle centered on the sun's disk to the area of that surface. If the plane is perpendicular to the axis of the solid angle, direct normal solar irradiance is received*".

This definition is simple to understand from a theoretical perspective, even though it remains vague due to the lack of specification about what a "*small solid angle*" actually is. This issue will be examined further in Section 2. The rest of this contribution is mainly concerned with the experimental side of the question.

Historically, the interest in accurate measurement of DNI started decades ago. Early studies (e.g., Linke, 1931; Linke and Ulmitz, 1940) identified the difficulty of separating the measurement of DNI from that of the diffuse irradiance in the immediate vicinity of the sun, hereafter referred to as *circumsolar irradiance*. Pastiels (1959) conducted a detailed study of the geometry of pyrheliometers, and how that geometry interacted with circumsolar radiance, using simplified representations of the latter. Various communications were then presented at a WMO Task Group meeting held in Belgium in 1966 (WMO, 1967) to improve the accuracy of pyrheliometric measurements, including estimates of the circumsolar enhancement. Ångström (1961) and Ångström and Rohde (1966) later contributed to the same topic, followed years later by Major (1973, 1980). The whole issue of instrument geometry *vs.* circumsolar irradiance was complex and confusing at the time because different makes and models of instruments had differing geometries. This was considerably simplified after WMO issued guidelines about the recommended geometry of pyrheliometers, which led to a relatively "standard" geometry used in all recent instruments. The experimental issues related to the measurement of DNI are discussed in Section 3.2.

After the theoretical background related to DNI in Section 2, a review of its multiple definitions, measurements and applications are reviewed in Section 3. Section 4 summarizes the expert consensus on clear definitions and terminology related to DNI. Section 5 gives examples based on simulations and ground measurements demonstrating the important role of circumsolar radiation in DNI, notably due to aerosols and thin clouds. Finally, Section 6 provides recommendations for a better mutual understanding of the possible definitions of DNI and how to reconcile them.

2. Theoretical background

Let $L(\xi,\varphi)$ be the broadband sky radiance—usually expressed in $\mathrm{W\,m^{-2}\,sr^{-1}}$—for an element of sky whose angular position is defined by the angular distance ξ from the center of the sun and its corresponding azimuth angle φ. The angle ξ is the angular distance of the considered point in the sky with respect to the angular position of the sun (Fig. 1). If the sun happens to appear within the sky patch considered, its radiance is included in L. The red surface is the plane perpendicular to the direction of the sun. The corresponding solid angle with aperture half-angle of ξ is represented by the grey cone.

Here, the term "*broadband*" refers to the shortwave part of the extraterrestrial solar spectrum that is received at the surface of the Earth, typically ranging from 290 to 3000 nm (WMO, 2010). This energy-rich part of the solar spectrum is covered by the spectral responses of pyrheliometers, which covers the range 300–4000 nm (e.g. EKO, 2011; Kipp and Zonen, 2008; Hukseflux, 2011). However, some CSP technologies with selective receiver coatings only use the spectral range from about 350 to 2500 nm (Benz, 2004). Similarly, PV and CPV collectors have a very different—narrower and uneven—spectral response than pyrheliometers. It should be noted that DNI is implicitly considered as broadband for this discussion.

The ISO definition of DNI, noted B_n, can be expressed by the following fundamental formula:

$$B_n = \int_0^{2\pi} \int_0^{\alpha_l} P(\xi,\varphi) L(\xi,\varphi) \cos(\xi) \sin(\xi) d\xi d\varphi. \quad (1)$$

where $P(\xi,\varphi)$ is the "penumbra function" that is sometimes also called "acceptance function". The penumbra function is equal to 0 for ξ greater than a limit angle α_l (see Section 3.2).

Sometimes, the aperture solid angle precisely defined by the penumbra function can also be simply or roughly characterized by an equivalent angular half width that may be called opening—or acceptance, aperture, viewing—half-angles.

The value of the penumbra function $P(\xi,\varphi)$ is defined by the fraction of parallel light rays incident on the aperture from the angles (ξ,φ) that reach the pyrheliometer's sensor element. The penumbra function can be calculated from the pyrheliometer's geometric specifications. For angles ξ_l

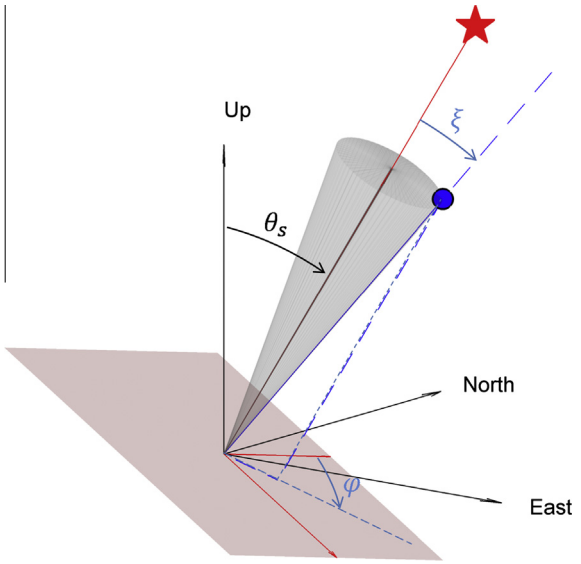

Fig. 1. Angular positions (ξ, φ) of a given point in the sky (circle), in the orthogonal spatial system defined by the direction of the sun (star). θ_s is the solar zenith angle. The red plane represents the plane perpendicular to the angular position of the sun, and the grey cone represents the solid angle of aperture half-angle ξ. (For interpretation of the references to color in this figure legend, the reader is referred to the web version of this article.)

less than 5°, the deviation from 1 of the $\cos(\xi)$ term can be considered negligible, so that Eq. (1) may be simplified into:

$$B_n = \int_0^{2\pi} \int_0^{\alpha_l} P(\xi,\varphi) L(\xi,\varphi) \sin(\xi) d\xi d\varphi. \quad (2)$$

Under the assumption of radial symmetry of the sky radiance in the vicinity of the sun position for clear skies (Gueymard, 1995, 2001; Buie and Monger, 2004), which can be considered reasonable when the sun is not too low over the horizon, Eq. (2) simplifies into:

$$B_n = 2\pi \int_0^{\alpha_l} P(\xi) L(\xi) \sin(\xi) d\xi \quad (3)$$

where $P(\xi)$ and $L(\xi)$ are the azimuthal averages of $P(\xi,\varphi)$ and $L(\xi,\varphi)$, such that:

$$P(\xi) = \frac{1}{2\pi} \int_0^{2\pi} P(\xi,\varphi) d\varphi \quad \text{and} \quad L(\xi) = \frac{1}{2\pi} \int_0^{2\pi} L(\xi,\varphi) d\varphi. \quad (4)$$

Gueymard (2001) provides an expression for $L(\xi)$ as a function of the aerosol optical mass, spectral Rayleigh and aerosol optical depths, aerosol phase function, and other variables. Eq. (3) outlines the way the DNI can be calculated from the azimuthal averages of the sky radiance and the penumbra function, in the vicinity of the sun, usually referred to as "*circumsolar region*" or "*aureole*".

The mathematical formulation of the definition for DNI, per Eq. (1), is ambiguous because neither a limit angle ξ_l nor a penumbra function is specified. This ambiguity is the main source of the multiple definitions of DNI found in the literature, since each of them explicitly or implicitly refers to different limit angles and penumbra functions, which inherently leads to varying amounts of integrated radiance in the vicinity of the sun.

When seen from outside the atmosphere, the sun appears basically as a disk whose angular radius can be quantified by the angular distance δ_s between the visible edge of the disk and its center. Considering the visible diameter of the sun ($\approx 1.392 \times 10^6$ km) and the varying sun-Earth distance during a year ($\approx 1.496 \times 10^8$ km $\pm 1.7\%$), δ_s is equal to 0.2666° $\pm 1.7\%$, using the set of constants from Liou (2002). In other words, at the top of atmosphere, the angular extent of the sun to be considered is defined by a limit angle equal to δ_s. At the ground level, due to scattering effects occurring within the atmosphere, the circumsolar region for angles greater than δ_s should be considered since its radiance is added to the radiance from the solar disk, typically up to 5° or more, depending on the application.

The direct radiance can be described as the radiance emanating from the circumsolar region and the sun. It is expressed as a function of the angular position relative to the center of the sun. The term *sunshape*, or $S_s(\xi)$, refers to the broadband azimuthal average radiance profile, normalized with respect to the radiance at the center of the sun, i.e.:

$$S_s(\xi) = K \int_0^{2\pi} L(\xi,\varphi) d\varphi \quad (5)$$

where the normalization constant K is determined so that $S_s(0) = 1$ (Biggs and Vittitoe, 1977).

As an example, Fig. 2 shows several sunshapes derived from the Lawrence Berkeley National Laboratory (LBNL)

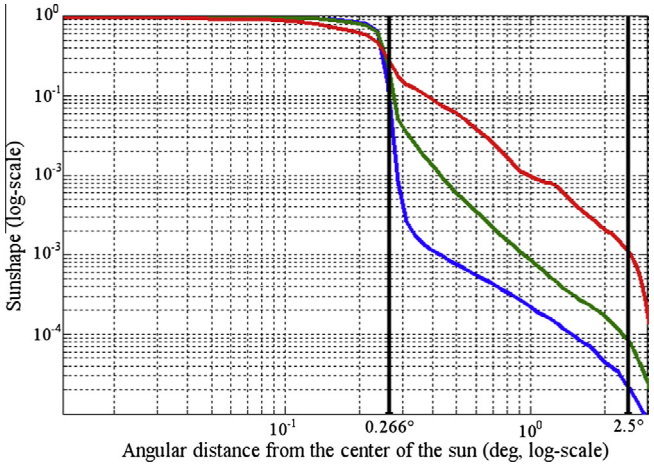

Fig. 2. Examples of sunshape profiles from the LBNL circumsolar telescope (Grether et al., 1975). The leftmost vertical thick black line indicates the edge of the solar disk and the rightmost one, the opening half-angle of a typical pyrheliometer.

circumsolar telescope (Grether et al., 1975; Noring et al., 1991).

Even without any influence of the terrestrial atmosphere, the solar disk radiance decreases with increasing angular distance from the center of the sun. This effect is referred to as limb darkening and varies with wavelength. While the radiance at the edge of the solar disk is approximately 55% of the radiance in the center of the sun at 1000 nm, the radiance decreases to approximately 20% at 370 nm. From the various limb-darkening models proposed in the literature, the radiance profiles presented by Pierce and Slaughter (1977) are recommended options to describe the region between 300 nm and 2400 nm.

3. Multiple definitions of DNI in the literature

The objective of this section is to review the multiple definitions and common acceptances related to DNI in different scientific fields, including radiative transfer in the atmosphere, radiometry, and solar energy conversion.

3.1. The strict definition for numerical modeling of radiative transfer in the atmosphere

The strict definition of the DNI refers to photons that did not interact with the atmosphere on their way to the observer.

The mathematical formulation of this fundamental definition of DNI, noted as B_n^{strict}, makes use of the broadband transmittance of the atmosphere T and the top-of-atmosphere—or extraterrestrial—normal irradiance E_n^{toa} for the actual sun-Earth distance (WMO, 2010):

$$B_n^{strict} = E_n^{toa} T \tag{6}$$

The broadband transmittance T depends on the altitude, solar zenith angle and parameters describing the optical state of the atmosphere related to aerosols, water vapor and other gases.

The definition of DNI described above is conceptually useful for atmospheric physics and radiative transfer models, but brings along a complication for ground observations or even for concentrating solar systems. It is not possible to identify whether or not a photon was scattered before it ultimately reaches an observing instrument. For the same reason, this strict definition also does not fit the ISO definition of DNI, since the ISO definition does not distinguish between scattered and non-scattered radiation.

Besides this fundamental problem, there are practical implications to consider too. Pyrheliometers have to track the apparent sun position along its path through the sky. As this cannot be done with perfect accuracy, pyrheliometers are designed such that they receive light from a greater angular aperture than the solar disk.

In the domain of numerical modeling of radiative transfer in the atmosphere with codes such as MODTRAN (Berk et al., 1998), SMARTS (Gueymard, 2001, 2005), or the publicly available solvers included in libRadtran

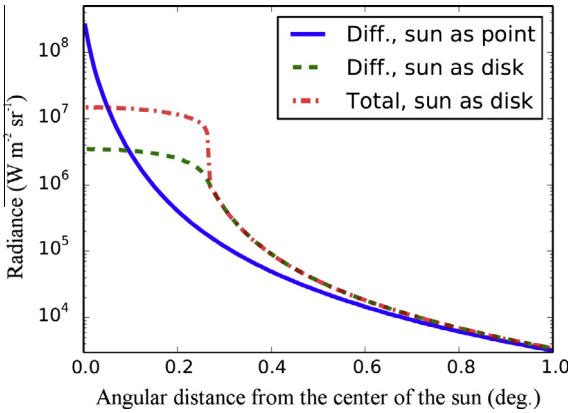

Fig. 3. Broadband radiance profile for a cirrus cloud (optical thickness of 0.5) and the sun in the zenith simulated with MYSTIC. Blue solid line: diffuse radiance for a point source. Green dash line: diffuse radiance for an extraterrestrial sunshape. Red dotted–dash line: direct and diffuse radiance for an extraterrestrial sunshape. (For interpretation of the references to color in this figure legend, the reader is referred to the web version of this article.)

(Mayer and Kylling, 2005), the direct normal irradiance is generally considered as a Dirac or delta function with no angular extent. DNI at the surface is modeled as the attenuation of the extraterrestrial radiation originating from the strict direction of the sun considered as a *point source*, without taking into account the scattered photons that may reenter the beam or the angular extent of the solar disk.

The very concept of numerical radiative transfer modeling that distinguishes non-scattered beam from scattered photons is currently evolving. For instance, within the EU-funded SFERA project, described by Reinhardt (2013) and Reinhardt et al. (2014), the authors have devised a special version of libRadtran, and modified the Monte-Carlo based radiative transfer equation solver named MYSTIC (Mayer, 2009) to account, *inter alia*, for a more realistic angular variation of the normalized extraterrestrial radiance over the solar disk. This solar radiance, hereafter referred to as "extraterrestrial sunshape", decreases from the center of the solar disk towards its edges, due to the phenomenon called "limb darkening" in solar physics, as mentioned above in Section 2. The extraterrestrial sunshape can also be modeled by other means to evaluate errors in spectral direct irradiance measurements obtained with sun photometers (Kocifaj and Gueymard, 2011).

Fig. 3 exhibits examples of simulated radial radiance profiles using either the extraterrestrial radiance modeled as a delta function (blue solid line) or with a realistic extraterrestrial sunshape (red dotted–dash line). In contrast, the green (dashed) curve represents the diffuse part of the radiance profile with a realistic extraterrestrial sunshape.

Because of constraints related to tracking accuracy and design-based limits on concentration factor, solar concentrating conversion systems also have different angular apertures, generally smaller than for pyrheliometers. Therefore, DNI is interpreted differently in the realm of solar energy and irradiance measurements than in the realm of radiative

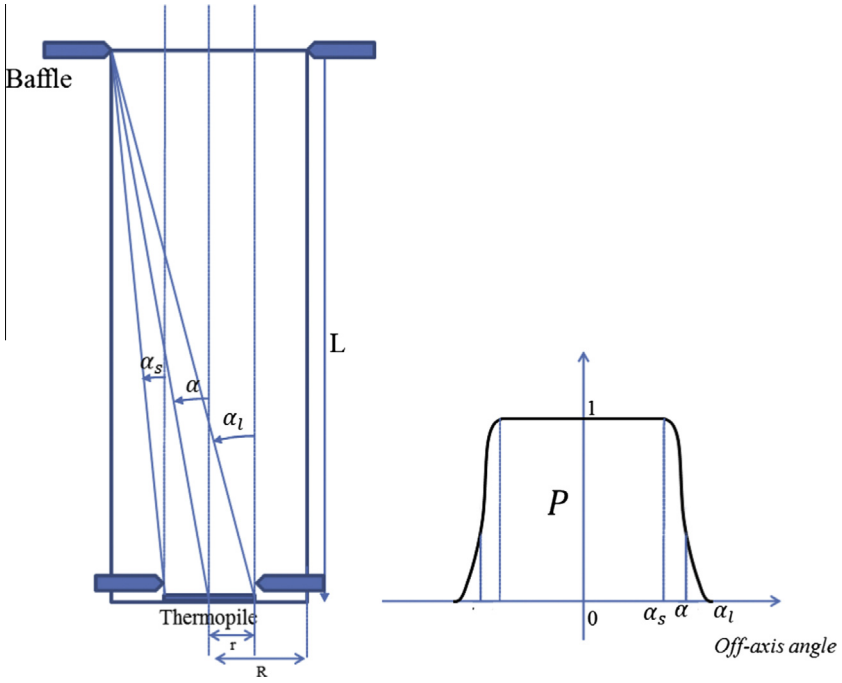

Fig. 4. Schematic representation of slope angle α_s, opening half-angle α and limit angle α_l of a circular opening pyrheliometer with the corresponding geometric penumbra function P with respect to the off-axis angle.

transfer modeling. Both interpretations of DNI are discussed in more detail in Sections 3.2 and 3.3.

3.2. The experimental definition for solar radiation measurement

The measurement of DNI is defined in the WMO CIMO Guide (WMO, 2010): "*Direct solar radiation is measured by means of pyrheliometers, the receiving surfaces of which are arranged to be normal to the solar direction. By means of apertures, only the radiation from the sun and a narrow annulus of sky is measured, the latter radiation component is sometimes referred to as circumsolar radiation or aureole radiation*".

This experimental definition is in a perfect agreement with the ISO definition of Section 3.1, and considers that DNI is logically related to the specific measurement device being used.

The amount of measured circumsolar scattered irradiance depends on the state of the atmosphere and on the specific penumbra function of the instrument (Pastiels, 1959). In most cases, this penumbra function can be approximated in a geometrical way by means of three angles: the opening half-angle α, the slope angle α_s, and the limit angle α_l (Fig. 4), defined as

$$\begin{aligned} \alpha &= a\tan\left(\frac{R}{L}\right) \\ \alpha_s &= a\tan\left(\frac{R-r}{L}\right) \\ \alpha_l &= a\tan\left(\frac{R+r}{L}\right) \end{aligned} \tag{7}$$

where R, r and L are characteristic dimensions of the instrument. Since these angles are usually small, their definition implies that:

$$\alpha \approx \frac{(\alpha_l + \alpha_s)}{2}. \tag{8}$$

Such a straightforward definition results in what is sometimes called the *geometric penumbra function* (Major, 1994). In practice, the numerical value of the penumbra function is given by the fraction of collected radiant flux by an optical aperture depending on the off-axis angles. The *effective penumbra function* is somewhat different from the geometric penumbra function, and obtained by taking into account effects such as the spatial inhomogeneity of the sensor in addition to its geometry (Major, 1994).

Penumbra functions for diffusometers—instruments consisting of a pyranometer with a shading disc or ball meant to shade the solar disc, so as to measure diffuse irradiance—are defined correspondingly, but refer to the fraction of rays that is blocked by a shading structure such as a tracking shade or a shadow ring, and thus does not reach the sensor (Major, 1992).

For off-axis angles between a minimum value of 0° and a maximum value equal to the slope angle α_s, the penumbra function is equal to 1. For angles greater than the limit angle α_l, the penumbra function is equal to 0. Finally, a continuously decreasing penumbra from 1 to 0 characterizes the range $[\alpha_s, \alpha_l]$. The opening half-angle α is the main characteristic for the description of the field of view of a pyrheliometer (Gueymard, 1998), and it corresponds approximately to the center of the transition range $[\alpha_s, \alpha_l]$. The viewing angle Ω is defined as the solid angle of a cone with apex angle 2α:

Table 1
Slope angle, opening half-angle, limit angle and viewing angle for several pyrheliometers, from Gueymard (1998) and data from manufacturers (EKO, 2011; Kipp and Zonen, 2008; Hukseflux, 2011; Middleton, 2008).

Brand, Model	Slope angle α_s (°)	Opening half-angle α (°)	Limit angle α_l (°)	Viewing angle Ω (sr)
Abbott, silver disk	0.8	2.9	4.9	8×10^{-3}
Eko, MS-56	1.0	2.5	4.0	6×10^{-3}
Eppley, AHF (cavity)	0.8	2.5	4.2	6×10^{-3}
Eppley, NIP	1.8	2.9	4.0	8×10^{-3}
Eppley, sNIP	0.8	2.5	4.2	6×10^{-3}
Hukseflux, DR01, DR02	1.0	2.5	4.0	6×10^{-3}
Kipp & Zonen, CH1, CHP1, SHP1	1.0	2.5	4.0	6×10^{-3}
Kipp & Zonen, Linke-Feussner	1.0	5.1	9.1	25×10^{-3}
Middleton, DN5, DN5-E	1.0	2.5	4.0	6×10^{-3}

$$\Omega = 2\pi(1 - \cos\alpha) \tag{9}$$

Of course, the opening half-angle—or the viewing angle—alone does not fully describe the penumbra function.

Table 1, based on Gueymard (1998), gives the value of such angles for common pyrheliometers.

The WMO CIMO guide (WMO, 2010) recommends an opening half-angle of 2.5° and a slope angle of 1°. Nevertheless, there is a large variety of pyrheliometers in current use (Rüedi, 2000; Gnos, 2010), which might have other geometries. Ångström and Rohde (1966) and Ångström (1961) studied a set of pyrheliometers with opening half-angles up to 10° and evaluated their typical circumsolar enhancement effects. Of course, different opening half-angles result in differing measured values. The instrument-to-instrument differences that the circumsolar effect generates are far from being negligible, especially in the presence of cirrus clouds. These differences must be seriously considered if the desired relative accuracy is better than 1.5%. In addition, several instruments have a circular aperture whereas others—however quite rare and old—have a rectangular aperture. The quasi-equivalence between the rectangular and circular field of view is valid ideally only for clear skies with low aerosol content (Willson, 1969).

The authors listed in the previous paragraph have underlined the need for further standardizing the acceptance conditions of pyrheliometers within meteorological networks. As a consequence, in 1978, the World Meteorological Organization (WMO) made the important decision that the radiometric definition of the Watt would have to be directly related to the electric scale through the World Radiometric Reference (WRR). The WRR is maintained experimentally by a group of stable instruments called active cavity radiometers (ACRs) located at the World Radiometric Center in Davos, Switzerland (WMO, 2010). This decision became effective on January 1, 1981 (Rüedi and Finsterle, 2005). The practical usage of WRR is described elsewhere (Gueymard and Myers, 2008). Every five years, an International Pyrheliometer Comparison (IPC) is conducted in Davos where the WRR reference instruments are used to transfer their calibration to other primary standards belonging to diverse countries. This process eventually trickles down and propagates in a way so that all calibrated field instruments in the world are ultimately traceable to the WRR. During the 11th IPC held in Davos in September–October 2010, an episode of Saharan dust occurred, which produced periods of slightly elevated dust aerosols in the air, in contrast with the normally very pure atmosphere at this elevation (1596 m). This circumstance provided an opportunity to study the effects of high-altitude aerosols on the transfer of calibration between instruments of different viewing geometries (Finsterle et al., 2012). Even though the necessary corrections were small (<0.1%), they were of similar magnitude as the stated WRR precision (≈0.1%) and uncertainty levels (≈0.3%). More details about the effect of circumsolar irradiance are provided in Section 5.

In the last few decades, other types of radiometer have started to be used for the purpose of measuring DNI as an alternative to conventional thermopile pyrheliometers. At the cost of an expected moderate loss of precision, these instruments can have some advantages, such as (i) lower first costs or investments; (ii) lower operation and maintenance costs; and (iii) decreased risks of misalignment, soiling or perturbation due to meteorological events, thus also decreasing down periods and maintenance costs. Examples of these alternative systems are:

- a pair of thermopile pyranometers, one unshaded to measure global irradiance and the other one equipped with a tracking shade (or, less desirably, a shadow ring), to measure diffuse irradiance;
- a thermopile radiometer resembling a pyranometer, but equipped with a system of shades inside the glass dome to separate the global and diffuse components (Wood, 1999);
- a rotating shadowband irradiometer (RSI) that alternatively senses the global and diffuse components at rapid intervals (Michalsky et al., 1986; Geuder et al., 2003, 2008, 2011; Vignola et al., 2012).

The determination of the DNI with these systems results from specific processing consisting of intermediate steps, such as:

- computation of the direct horizontal irradiance from the difference between the measured global and diffuse horizontal irradiances;

- computation of DNI from direct horizontal irradiance by dividing it by the cosine of the solar zenith angle;
- corrections for RSI systems to compensate for systematic errors (e.g. King et al., 1998; Geuder et al., 2003, 2008, 2011; Vignola, 2006);
- corrections needed to compensate for the shaded part of the sky when using a shadow ring or other system of shades (e.g. WMO, 2010; López et al., 2004; Batlles et al., 1996).

The opening half-angles that would characterize the measured DNI when using these alternative pyranometric systems are not always easy to define. Indeed, they depend on the sensor-sun geometry and on the specific procedure used to calibrate the instrument against a reference pyrheliometer or ACR. Additionally, the variability of the irradiance measured during the rotation of the shadowband of a RSI has to be considered (Wilbert et al., 2012; Wilbert et al., 2013c).

The accuracy of some of these instruments or methods is limited and may not even be adequate to successfully distinguish the effects and differences stated above.

An inter-comparison of such alternative sensors from different manufacturers has been made in Payerne (Switzerland), in the frameworks of the European COST program (cooperation in science and technology) ES1002 WIRE (weather intelligence for renewable energy) and IEA SHC Task 46. The results of this DNI inter-comparison will be published soon.

Sensor soiling has an additional impact on the experimental determination of DNI. It should be avoided as thoroughly as possible during measurement campaigns since its impact may easily outweigh the effects of circumsolar radiation or of differing instrument geometries. Since soiling cannot always be avoided, its effect on the uncertainty of DNI measurements should be quantified along with the measurements. The effects of instrument soiling are strongly dependent on site, instrument type, season and corresponding weather and environmental conditions (Geuder and Quaschning, 2006). Mitigation measures require a meticulous record of the sensor cleanings with their exact times and the potential increase in the corresponding sensor signal along with signal coincidence in the case of redundant measurements. Such methods are described in (Geuder and Quaschning, 2006; Pape et al., 2009; Wolfertstetter et al., 2012; Wolfertstetter et al., 2013).

3.3. The practical usage in solar energy conversion

3.3.1. Overview of power plant performance models

Circumsolar radiation and the corresponding sunshape play a role in determining the efficiency of concentrating solar systems, and are always somehow—and sometimes implicitly—included in common solar performance models. Such models include ray tracing tools, analytical optical performance models, and models that determine the optical performance with look-up tables or parameterizations of the solar position relative to the collector. To better understand the use of the term DNI in power plant models we briefly introduce different types of optical performance models and tools.

- *Ray tracing models*

The available solar radiation can be described as a multitude of solar rays transmitted from the sun to the concentrators and finally to the receiver. Ray tracing tools such as STRAL (Belhomme et al., 2009), SolTRACE (Wendelin, 2003), MIRVAL (Leary and Hankins, 1979), or SPRAY (Buck, 2010) calculate the path of the sun's rays from the sunshape to the receiver by application of physical laws. Monte Carlo techniques are often implemented to allow for tractable calculation times.

For the sake of illustration, one method for the description of the sunshape that is available in SPRAY is explained in the following. The method selects one concentrator element after another and traces a given number of rays from the current element. After the calculation of the vector to the center of the sun, the appropriate sunshape is included. This is done by calculating an angular deviation of the ray vector from the center of the sun based on the probability density function corresponding to the sunshape as defined in Section 2.

To do so, a user-defined sunshape has to be provided as an input to SPRAY. The radiance is determined both by the specified DNI and the user-defined sunshape. The specific ray under scrutiny is then related to a power calculated as the product of the incident DNI and the projected area of the current concentrator element divided by the number of rays per element. Then the path of the ray is followed until it reaches the receiver.

This ray tracing method can be based on actual measurements of the plant geometry.

- *Analytical optical performance models*

The Bendt–Rabl model (Bendt et al., 1979; Bendt and Rabl, 1981) is another type of calculation method that uses an analytical approach. To accelerate calculations, analytical equations are derived and solved to describe the ray's path through the optical system. For instance, the model suggested by Bendt and Rabl can be used for parabolic troughs and solar dishes. In a first step, an angular acceptance function is determined from the design geometry. The angular acceptance function $P_{acc}(\alpha)$ is defined by the fraction of rays incident on the aperture at an angle α that reaches the receiver. This is equivalent to the definition of the penumbra function given in Section 2.

The second step of the Bendt–Rabl method is to determine an effective source that includes both the user-defined sunshape and the deviations from the design geometry. The optical errors of a CST collector are described as Gaussian-distributed independent uncertainties. Their combination is

also a Gaussian distribution with standard deviation σ_{opt}, which is often called *optical error*. The function that describes the optical errors is then combined with the sunshape using convolution. For line-focusing systems, such as parabolic troughs, a further integration step is required because the effect of circumsolar radiation on the incident irradiance depends strongly on angle φ (Eq. (1)).

Finally, the intercepted radiation can be determined by integrating the product of the effective source and the acceptance function, similar to Eq. (3).

Bendt and Rabl (1981) also describe an alternative order of the calculation steps that combines the angular acceptance function and the optical errors to the so-called "smeared acceptance function", which is then combined with the sunshape.

Similar analytical methods are used in HELIOS (Vittitoe and Biggs, 1981), DELSOL (Kistler, 1986) and HFLCAL (Schwarzbözl, 2009).

- *Look-up tables-based optical performance models*

The fastest way to determine the optical performance of a CST collector uses only parameterizations or look-up tables that describe the change of the optical performance with solar position. The necessary parameters can be derived from experimental data, or the aforementioned analytical performance models or raytracing tools. Experimental measurements are obtained for a given time series of sunshapes. In contrast, results from the aforementioned models always have to make assumptions concerning the sunshape. Hence, even such simple performance models indirectly include an assumed sunshape. Only one constant sunshape is typically described by these simple models, which may constitute a serious limitation. As a rather extreme example that can occur when thin clouds mask the sun, Grether et al. (1977) found 15% and 24% reduction of the intercept factor for two solar towers using a broad sunshape with a CSR of 0.4.Such look up tables or parameterizations are used in SAM (Gilman et al., 2008) and Greenius (Quaschning et al. 2001; Dersch et al., 2011).

3.3.2. Definition of the required input DNI for performance models

The first two types of model mentioned above—ray tracing and analytical models—need the sunshape and DNI as input variables. The third model type (look-up tables) only requires DNI as input, whereas assumptions on the sunshape are included as fixed settings in the model.

In CST applications, the term DNI is commonly interpreted as the experimental DNI that is measured with a pyrheliometer. This does not always lead to the right interpretation of the plant performance analysis software, however. For the ray tracing tool SPRAY, for instance, the input DNI value is related to rays that are distributed over the complete interval up to the angle ξ_l over which the sunshape is defined by the user. The input DNI must be computed by the user from the chosen sunshape and experimental DNI, provided that the angle ξ_l is greater or equal to the limit angle of the pyrheliometer.

Users must pay attention to the adequacy between the limit angle of their user-defined sunshape and the limit and slope angles of the pyrheliometer considered as the source of the experimental DNI. For instance, the experimental sunshapes presented by Neumann et al. (2002) all have the same limit angle of 1.72°, which makes them incompatible with experimental DNI data obtained with common pyrheliometers having a 2.5° opening half-angle. In contrast, the standard solar scan (Rabl and Bendt, 1982) is defined up to 3.2°. Hence, the error due to the angular incompatibility is smaller in the later case, since only the angular interval from 3.2° to the limit angle is affected. The same holds for the sunshapes proposed by Buie et al. (2003b).

Rabl and Bendt (1982) discuss the interaction between the specified DNI and the outer limit angle (up to an angle of 3.2°) of the sunshape data used in their study. They define the optical performance of a solar system for the specific penumbra function of the Eppley Normal Incidence Pyrheliometer (NIP), which has an opening half-angle of 2.9° (Table 1). The optical performance that is obtained after the above-explained convolutions and spatial integration is hence only a preliminary result. This preliminary result refers to an angle of 3.2° that coincides with the limit of the LBNL circumsolar radiance data and not to the penumbra function of the pyrheliometer. Rabl and Bendt (1982) derived the experimental optical performance by multiplying this preliminary result with the ratio of DNI computed with the sunshape with a 3.2° opening half-angle and perfect penumbra function and the measured DNI.

For performance models that use look-up tables or experimental data, DNI has to be defined in correspondence with the source of the parameters or look-up table. For such models, however, errors may occur if the sunshape deviates from the indirectly included sunshape of the parameters or look-up table.

Although two of the three aforementioned types of performance model allow calculations with arbitrary user-defined sunshapes, typically only constant standard sunshapes are used. Nevertheless, Wilbert (2014) has processed time series of sunshapes using a software add-on for SPRAY. For the processing of DNI time series from typical meteorological years, however, no approach for the corresponding sunshape data is published so far. Further research is thus required to alleviate the lack of site-specific sunshape data for such applications.

3.3.3. Approximation of the angular acceptance of CST collectors with acceptance angles

The availability of site-specific time series of both the experimental DNI and corresponding sunshape is the ideal case in CST modeling. Approximate descriptions of the collector performance including the variation of circumsolar radiation might be achieved by specifying a collector-specific DNI (Lemperle, 1982) that only includes radiation

up to a collector-specific outer boundary angle, which is called acceptance angle. Such approximations and their shortcomings are not the topic of this paper. What is described here is rather an overview of definitions and values of acceptance angles that might be adequate for such approximations, as an illustration of the contribution of circumsolar radiation to collector performance.

Several concentrating solar systems exist with different types of collectors having diverse apertures corresponding to different limit angles ξ_l and penumbra functions. These are generally not the same as the apertures characterized by pyrheliometers or other DNI measurement devices.

In the domain of solar energy conversion, the term "acceptance half-angle" is generally used instead of "opening half-angle". The nominal acceptance angle is defined in (Rabl, 1985) as "*the largest incidence angle for which all or almost all rays on the aperture reach the receiver*" and can be roughly considered as analog to the slope angle for pyrheliometers. Other approaches can be cited to define an equivalent acceptance angle, such as the one also proposed by Rabl (1985), which is obtained as twice the standard deviation of the radiation angular distribution incident on the absorber. The acceptance half-angle can be also defined as the off-axis angle at which the sensitivity of the instrument decreases below a given fraction of the incident irradiance, e.g. 50% or 90%.

The nominal acceptance half-angle of a concentrating collector and its concentration factor are closely related. This relation depends on the quality of the non-imaging collecting optical system. Calling upon the second law of thermodynamics, Rabl (1976) demonstrates the existence of an upper bound of the concentration factor C for a given acceptance half-angle θ_c. For a refraction index of the solar concentrator equal to 1, one obtains:

$$C \leqslant \frac{1}{\sin(\theta_c)^d} \tag{10}$$

where d equals 2 for point focusing collectors (e.g. parabolic dish or solar tower) and 1 for line focusing collectors (e.g. parabolic through or linear Fresnel).

As stated above, we do not discuss the application of the acceptance angles for CST modeling or the quality of such models, but only state the upper bounds for acceptance angles as an illustration.

To illustrate the diversity of the possible acceptance angles in CST systems, we have collected the concentrating factors and acceptance angles of several systems from the literature.

Table 2 shows typical concentration factors of various CSP technologies (IRENA, 2012) and the corresponding upper bound of acceptance half-angles from Rabl (1976). These upper bounds are within the typical range 0.7–2.3°, and are typical of concentrating collectors such as parabolic through, solar tower or parabolic dish (Meyen and Lüpfert, 2009).

In parallel, Table 3 provides data on the concentration factors and their corresponding upper bounds of acceptance half-angles for several CPV systems, assuming a refraction index of the solar concentrator equal to 1.

4. Expert consensus on DNI definitions in the framework of IEA SHC Task 46

The need for clear and specific definitions and terminology related to DNI was raised by MINES ParisTech (Blanc et al., 2013) in the name of the EU-funded MACC-II project, in the framework of two expert meetings and dedicated workshops under IEA SHC Task 46: "*Solar Resource Assessment and Forecasting*". Approximately 70 experts from 12 countries participate in Task 46.

As an outcome of discussions held at Task 46 Expert Meetings and workshops during 2012–2013, various definitions related to DNI were specified with their corresponding acronyms. The following is a synthesis of these conclusions.

In the ideal case where the penumbra function is a perfect rectangular function with respect to the off-axis angle (i.e. no transition range), an ideal DNI for the opening half-angle α, named $B_n^{ideal}(\alpha)$, is defined as follows:

$$B_n^{ideal}(\alpha) \approx 2\pi \int_0^{\alpha} L(\xi)\sin(\xi)d\xi. \tag{11}$$

The direct irradiance from the sun, noted B_n^{sun}, is defined as the solar radiant flux collected by a surface normal to the direction of the sun, within the current extent of the solar disk only (half-angle δ_s) with a perfectly rectangular penumbra function. This constitutes a special case of Eq. (11), with $\alpha = \alpha_s = \alpha_l = \delta_s$ and:

$$B_n^{sun} = B_n^{ideal}(\alpha = \delta_s) \approx 2\pi \int_0^{\delta_s} L(\xi)\sin(\xi)d\xi. \tag{12}$$

With this definition, used by Buie et al. (2003a) for instance, the small fraction of diffuse radiance within the solar disk is included. Theoretically, B_n^{sun} is different from B_n^{strict} because the latter consists only of non-scattered radiant flux. In practice, however, the difference between the

Table 2
Upper bounds of acceptance half-angles from Rabl (1976) for typical concentration factors of different CSP technologies, as described in the IRENA working paper (IRENA, 2012).

CSP Types	Dish-Stirling	Solar tower	Parabolic through	Linear Fresnel
Concentration factor	>1300	>1000	70–80	60
Dimensional concentration type	3-D	3-D	2-D	2-D
Upper bound of acceptance half-angles from Rabl (1976)	<1.6°	<1.8°	<0.8°	1°

Table 3
Concentration factors and corresponding upper bound acceptance half-angles for different solar concentrating photovoltaic (CPV) systems. *Source:* http://techtransfer.universityofcalifornia.edu/NCD/10320.html (last accessed 05.12.14).

CPV Types	Concentration factor	Upper bound of acceptance half-angles (°) from Rabl (1976) (°)
Two aplanatic mirrors + homogenizing prism	500	<2.6
Total internal reflection + refractive secondary optics	1000	<1.8
Polymethylmethacrylate dome-shaped Fresnel lens + glass kaleidoscope	550	<2.4
Fresnel lens + reflective inverted pyramid secondary	250	<3.6

two quantities corresponds to the spatial integration of diffuse radiance within the solar radius angle, which can be considered negligible.

In the more general—and concrete—context of DNI measurements or solar conversion systems, the penumbra function P is generally not a perfect rectangular function.

The limit angle α_l is defined as the angle above which the acceptance function is null or considered as negligible:

$$\forall \xi \geqslant \alpha_l P(\xi) \approx 0. \tag{13}$$

This limit angle α_l is the greatest angular distance from the center of the sun that is considered to be part of the circumsolar region, for a given acceptance function P. The angular extent of this circumsolar region cannot be defined in a universally valid way. This is due to the fact that different pyrheliometers and different concentrating collectors are sensitive to radiance up to specific angular distances from the center of the sun.

For example, the limit angle α_l is 3.2° for the measured circumsolar ratio (CSR) in the LBNL data base (Noring et al., 1991). For pyrheliometer measurements following the WMO recommendations (WMO, 2010) a limit angle greater than 4° would be necessary.

The slope angle α_s is defined as the angle below which the penumbra function equals 1, or its deviation from 1 can be considered negligible:

$$\forall \xi \leqslant \alpha_s P(\xi) \approx 1. \tag{14}$$

The experimental definition of DNI for an acceptance function P and its limit angle α_l defined by Eq. (3) can then be related to the ideal DNI for the opening half-angle α_s:

$$B_n \approx B_n^{ideal}(\alpha_s) + 2\pi \int_{\alpha_s}^{\alpha_l} P(\xi) L(\xi) \sin(\xi) d\xi. \tag{15}$$

Under the (reasonable) assumption that the acceptance function P is equal to 1 for off-axis angles less than the solar disk half-angle δ_s, it is clear that $\delta_s \leqslant \alpha_s$, hence the following relationship is obtained:

$$B_n \approx B_n^{sun} + 2\pi \int_{\delta_s}^{\alpha_l} P(\xi) L(\xi) \sin(\xi) d\xi. \tag{16}$$

The experimental circumsolar normal irradiance, CSNI, noted CS_n, is related to the acceptance function P, and is defined as the part of the corresponding DNI that is incident from the annular angular region defined by the two half-angles α_0 and α_1 verifying the constraint $\delta_s \leqslant \alpha_0 \leqslant \alpha_1 \leqslant \alpha_l$:

$$CS_n(\alpha_0, \alpha_1) \approx 2\pi \int_{\alpha_0}^{\alpha_1} P(\xi) L(\xi) \sin(\xi) d\xi. \tag{17}$$

Following Eq. (16), a fundamental closure relationship is obtained:

$$B_n = CS_n(\delta_s, \alpha_1) + B_n^{sun}. \tag{18}$$

Similarly to the ideal DNI, the ideal CSNI, noted CS_n^{ideal}, is defined as the part of ideal DNI coming from the annular angular region defined by the two half-angles α_0 and α_1 verifying the order constraint $\alpha_0 \leqslant \alpha_1$:

$$CS_n^{ideal}(\alpha_0, \alpha_1) \approx 2\pi \int_{\alpha_0}^{\alpha_1} L(\xi) \sin(\xi) d\xi. \tag{19}$$

Similarly to Eq. (18), the following relationship is then obtained:

$$B_n^{ideal}(\alpha) = CS_n^{ideal}(\delta_s, \alpha) + B_n^{sun}. \tag{20}$$

The circumsolar ratio (CSR) for the opening half-angle α, noted $CSR(\alpha)$, is then defined as the ratio between the ideal CSNI for $\alpha_0 = \delta_s$ and $\alpha_1 = \alpha$ and the ideal DNI $B_n^{ideal}(\alpha)$:

$$CSR(\alpha) = \frac{CS_n^{ideal}(\delta_s, \alpha)}{B_n^{ideal}(\alpha)}. \tag{21}$$

Eq. (21) is used in the literature to describe the circumsolar ratio (Grether et al., 1977; Schubnell, 1992; Neumann and Witzke, 1999). Depending on the authors and the measurement systems, other angles are used for δ_s. For instance, Neumann and Von Der Au (1997) use the *current* solar disk angle plus 0.0206° (0.36 mrad) for sunshape measurements, in order to avoid the effect of imperfect image sharpness of the experimental images. Alternatively, in Neumann et al. (2002), the *average* solar disk angle 0.2664° (4.65 mrad) is used for average sunshapes, thus introducing a small error—less than 1.7%—caused by neglecting the annual variation of the solar disk angle due to the elliptic path of the Earth around the sun. LBNL used the current solar disk angle increased by 0.013° as the inner limit angle to avoid instrumental errors that could cause an overestimation of the radiance close to the solar disk edges (Grether et al., 1975).

Buie et al. (2003b) showed that CSR characterizes the sunshape to some extent. However, there is no bijective relation between the sunshape and CSR. Indeed, a specific value of CSR can be obtained for different sunshapes, as discussed by *e.g.* Wilbert et al. (2013b).

Finally, and in a similar way, the circumsolar contribution (CSC) from a given annular region can be defined as

$$CSC(\alpha_0,\alpha_1)=\frac{CS_n^{ideal}(\alpha_0,\alpha_1)}{B_n^{ideal}(\alpha_1)}. \quad (22)$$

5. Circumsolar radiation and its effect on DNI

The circumsolar irradiance and its angular distribution are dependent on the physical characteristics of aerosols and thin clouds—most particularly optically thin cirrus clouds—in the atmosphere. Whenever thin clouds obscure the sun, important modifications to the underlying clear-sky circumsolar irradiance will occur, because clouds have different optical characteristics than aerosols. This section uses both real measurement-based and simulated examples to demonstrate that the amount of circumsolar radiation and its relative contribution to the measured or simulated DNI varies strongly with sky condition.

SMARTS simulations for clear-sky conditions with various loads of *rural aerosols*, composed of small aerosol particles, have shown that, for relatively low θ_s, the relative proportion of the circumsolar irradiance in the measured DNI is less than 1% for opening half-angles ranging from 2.5° to 2.9° (Gueymard, 2010a,b). Increasing the air mass from 1 ($\theta_s = 0°$) to 3 ($\theta_s = 70.7°$) roughly results in the doubling of the circumsolar contribution. For the specific conditions of the ASTM G173 reference spectral standard, which is used by the PV and CPV communities for rating purposes, the combination of an air mass of 1.5 ($\theta_s = 48.24°$), a rural aerosol with an aerosol optical depth (AOD) of 0.084 at 500 nm, and other atmospheric conditions defined in the standard, similar SMARTS calculations indicate a circumsolar contribution of only 0.25% for a 2.9° aperture half-angle. For many aerosol types composed of small particles and/or not too large AOD, the circumsolar contribution is essentially proportional to the slant optical depth (SOD) defined as the product of AOD and air mass, so that an AOD of 0.084 at air mass 15, or an AOD of 0.84 at air mass 1.5, would induce a circumsolar contribution 10 times greater than before, or approximately 2.5%. In the specific case of small aerosol particles and opening half-angles α less than 10°, the circumsolar contribution to DNI is found to vary almost linearly with α (Gueymard, 2010a,b). These SMARTS results have been validated against more rigorous calculations of spectral circumsolar irradiance (Gueymard, 2001; Kocifaj and Gueymard, 2011).

In addition to the SOD, the scattering phase function is the other dominating factor that governs the magnitude of the circumsolar contribution. The scattering phase function can be defined as the intensity of electromagnetic radiation at a given wavelength that is scattered for a given angle from the original direction of the incident beam (Zdunkowski et al., 2007). The scattering phase function depends on the type of aerosol or cloud particles (material, particle size and shape). Large particles, such as desert dust particles or ice crystals, tend to scatter more strongly in the close vicinity of the forward direction than smaller particles such as rural aerosol particles, thus yielding comparatively larger circumsolar contributions. Under cloudless skies, and for a given value of the SOD, this means that the circumsolar contribution would be normally larger over arid/desert areas than over rural areas.

The principle just stated that "larger particles induce greater circumsolar radiation" only holds for aerosols. In the case of cirrus clouds, ice particles may be so large that the forward scattering peak becomes extreme and the scattering angles for most photons can be smaller than the angular extent of the sun disk itself. This increases the diffuse radiation coming from the part of the sky occupied by the sun disc, but may lead to smaller circumsolar radiance values than in the case of smaller particles. In such extreme cases, a brighter sun disc but dimmer circumsolar region leads to smaller CSR values.

For the sake of illustration, simulations of the circumsolar radiation for an opening half-angle of 2.5° have been performed with a specifically modified version of the MYSTIC Monte Carlo radiative transfer model that allows, notably, a precise description of the extraterrestrial sunshape to be considered (Reinhardt et al., 2014; Mayer, 2009). To cover the full range of expected circumsolar radiation values while maintaining conciseness and legibility, only results for sky conditions resulting in specifically high or low circumsolar radiation values are shown in the following. Cirrus clouds are represented using the optical properties of Hong-Emde-Yang (Reinhardt et al., 2014) for rosettes and solid columns with effective radius of respectively 90 μm and 15 μm. The former size yields low circumsolar radiation values in the considered 2.5° field-of-view, whereas the latter yields high circumsolar radiation values. As far as aerosols are concerned, three aerosol types have been chosen from the optical properties of aerosols and clouds database (OPAC) proposed by Hess et al. (1998):

- The continental polluted aerosol type is composed of mostly small particles and causes low circumsolar radiation values even for high AOD values. This aerosol type is typical over areas highly polluted by anthropogenic activities;
- The desert aerosol type contains a significant amount of large aerosol particles and therefore induces considerably more circumsolar radiation;
- A coarse aerosol type, obtained as the pure coarse mineral dust component from OPAC minus the smaller particles. This third type has been considered because it may induce circumsolar radiation with the

same magnitude as cirrus clouds, even though situations where only large particles exist are highly unlikely. This somewhat unrealistic type of aerosol is introduced here to demonstrate that, over desert regions, it is not easy to define an upper limit for the circumsolar radiation caused by aerosols since local uptake may cause a particle size distribution that contains considerably more large particles than in the average OPAC desert dust mixture.

The different simulations were performed for five different values (0.1, 0.2, 0.3, 0.4 and 0.6) of the vertical optical depth at 550 nm τ_{550}, and for different sun zenith angles from 0° to 80° in steps of 10°. These simulations are derived with the same methodology as that presented by Reinhardt et al. (2014).

The SOD at 550 nm, noted d_{550}, is defined by:

$$d_{550} = \frac{\tau_{550}}{\cos\theta_s}. \quad (23)$$

Fig. 5(a) and (b) respectively show the ideal CSNI and the corresponding ideal CSR for an opening half-angle of 2.5°, as a function of d_{550}. It is found that CSR is a strong function of d_{550}. However, Fig. 5(a) shows that CSNI also depends on the sun zenith angle, since there are several combinations of vertical optical depth and sun zenith angle that yield similar values of d_{550}.

Using the same MYSTIC simulations, Fig. 6 shows the correspondence between $CSR^{ideal}(2.5°)$ and $B_n^{ideal}(2.5°)$. For

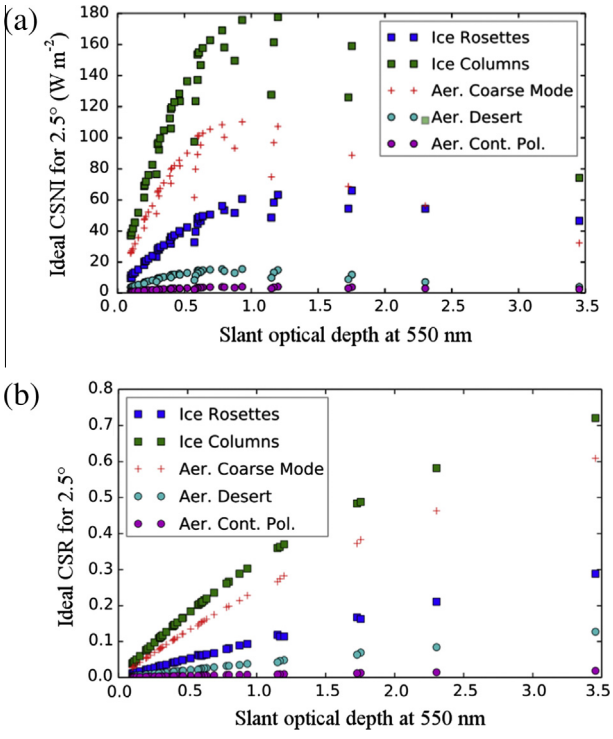

Fig. 5. Simulations with libRadtran/MYSTIC of scattering effects of different types of aerosol and ice cloud on the CSNI $CS_n^{ideal}(2.5°)$ (a) and on the circumsolar ratio $CSR^{ideal}(2.5°)$ (b).

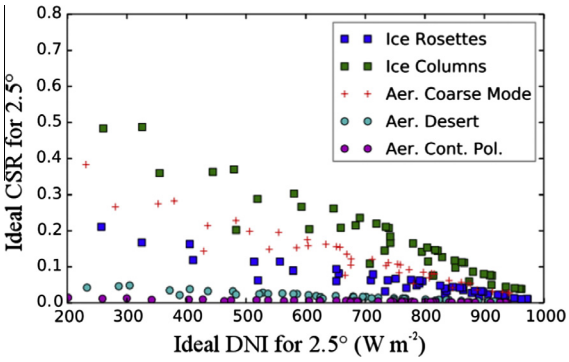

Fig. 6. Simulations with libRadtran/MYSTIC of scattering effects of different types of aerosol and ice cloud on $CSR^{ideal}(2.5°)$, together with $B_n^{ideal}(2.5°)$.

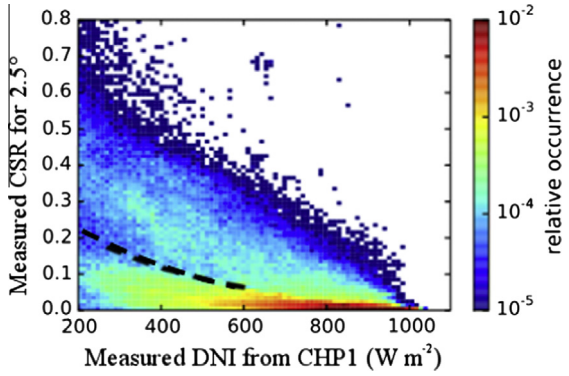

Fig. 7. 2D histogram composed of measurements of the $CSR(2.5°)$ and the corresponding experimental DNI, B_n. These measurements come from respectively a SFERA sunshape measurement system and a CHP1 pyrheliometer installed at the *Plataforma Solar de Almeria* (Spain).

the same magnitude of simulated DNI, different circumsolar ratios can be observed with respect to the aerosol or ice-cloud types, which means that the circumsolar contribution to DNI is not just a function of turbidity. Small circumsolar ratios correspond to aerosols under clear-sky conditions, whereas large ratios correspond to cloudy-sky conditions with ice clouds.

Fig. 7 presents a combined two-dimensional (2D) histogram of measurements of the circumsolar ratio and DNI performed at the *Plataforma Solar de Almeria* (Spain) using the so-called SFERA sunshape measurement system. This SFERA system consists of Visidyne Sun and Aureole Measurement System (SAM), a Cimel sun photometer, a CHP1 pyrheliometer, and appropriate post-processing software (Wilbert et al., 2013a). The 2D histogram in Fig. 7 has been created from 337,701 measurements taken between April 1st 2011 and December 20th 2012.

These measurements corroborate the MYSTIC simulations presented in Fig. 6. The histogram contains a "bend", represented by a black-dashed line in Fig. 7 for lower DNI values, which is interpreted as a signature of the transition between cloudless and cloudy conditions. Measurements below this 'bend" for lower CSR values correspond to clear-sky measurements with typically small aerosol particles.

A very practical analysis of these simulation- or measurement-based figures shows situations or conditions with high experimental DNI together with high circumsolar ratios. For example, for an experimental DNI around 600 W m^{-2}, for approximately 7% of the situations, the circumsolar ratios reach 20–30%, due to the effect of thin clouds. This implies that a solar energy conversion system with a narrow acceptance angle—just slightly greater than δ_s—would be able to convert only 70–80% of the experimental DNI under such circumstances.

Aerosols also cause an increase in the relative difference between $B_n^{ideal}(\alpha)$ and B_n^{sun}, but, conversely to the effect of cirrus clouds, their effect may strongly decrease $B_n^{ideal}(\alpha)$.

This difference in how aerosols and thin clouds impact DNI is caused by the Ångström exponent η that characterizes the variation of spectral AOD with wavelength in Ångström's law:

$$\tau(\lambda) = \tau(1\ \mu m)\lambda^{-\eta} \tag{24}$$

where $\tau(\lambda)$ is the AOD at wavelength λ (in μm).

For instance, rural aerosols have an exponent that usually ranges between 1 and 1.5, which means that the extinction in the visible band—where the spectral irradiance is high—is much stronger than in the near infrared (where the spectral irradiance is much lower). In comparison, the scattering effect of clouds is roughly wavelength independent ($\eta \approx 0$), and is therefore generally of lower magnitude in the ultraviolet and visible parts of the spectrum than that of aerosols for a similar optical depth. However, this difference would become almost non-existent under sand storm conditions, because the overwhelming presence of large particles would make the aerosol Ångström exponent η reach values close to 0.

6. Conclusions and recommendations

Depending on atmospheric conditions, a more or less significant fraction of solar radiation that is scattered by atmospheric constituents emanates from the circumsolar region. Whereas a large part of the circumsolar radiation is measured by pyrheliometers, concentrating collectors can only use a part of it, depending on concentrator technology, among other things. Therefore, this circumsolar effect has to be considered for yield assessment and performance evaluation of concentrating solar technologies.

Given these circumstances, circumsolar radiation measurements or estimates should be included in solar resource assessment, plant design, yield assessment, plant operation, or power plant performance tests for concentrating technologies. Otherwise, an additional uncertainty is introduced. In parallel, standard DNI measurements using procedures that follow the WMO-recommended geometry—in terms of slope and limit angles—always need to be carried out for solar resource assessment and performance monitoring.

An early study (Lemperle, 1982) suggested that a pyrheliometer with a modified opening angle similar to the CST system's acceptance angle could be used as an alternative to sunshape measurements. Although there could be a market for "special geometry" pyrheliometer, such an approach cannot be recommended for five reasons. First, the acceptance angle is specific to each CST system technology. Hence the DNI assessment should be system specific, too, which is difficult and costly to implement in practice. Second, such an approach is only an approximation even for a single specific system. Third, the sensitivity of a CST to circumsolar radiation varies with solar position for all types of systems except for parabolic dishes. Fourth, any deviation from the WMO recommendation for the geometry of pyrheliometers brings along a complication when comparing data from these measurements to data obtained with conventional, WMO-compliant instruments. Fifth, the calibration of pyrheliometers of unusual geometry becomes more uncertain since this calibration is obtained by comparing their reading to reference instruments (ACRs) that have a mandated 2.5° opening angle, with no adjustment possible.

The last two reasons, related to the geometry of radiometers, also apply to the case of modeled data, since radiation models are usually validated, and sometimes also partially calibrated, against standard ground-based measured DNI data.

The authors strongly recommend that standard DNI measurements following the WMO-recommended field of view be conducted at all radiometric stations. Such measurements can be collected with pyrheliometers, of course, but also e.g. with RSIs or dual pyranometers, since these are calibrated against common pyrheliometers. If possible, circumsolar radiation measurements should also be carried out in addition to the common DNI observations.

In the best-case scenario, circumsolar radiation measurements can be reduced to sunshape functions. However, the measurement of the circumsolar ratio or of the circumsolar contribution may be sufficient, depending on conditions and applications.

As a guideline for the proper usage of the term "DNI" we conclude with the following:

- Different interpretations of the term DNI are required depending on the topic and scientific field.
- A decision to establish a *single* interpretation of the term DNI is neither necessary nor possible.
- To allow for the correct interpretation of published results, and in order to avoid introducing additional errors, it is necessary to explain clearly which definition of DNI is used. In the case of experimental DNI data, this involves the specification or the characterization of the penumbra function.

Acknowledgements

This paper has been done in the framework of the IEA SHC Task 46 "Solar Resource Assessment and

Forecasting", in collaboration with both the IEA SolarPACES and IEA PVPS implementing agreements.

The research leading to these results has partly received funding from the European Union's Seventh Framework Programme (FP7/2007-2013) under Grant Agreement No. 283576 (MACC-II project, Monitoring Atmospheric Composition and Climate-Interim Implementation) and grant agreement no. 228296 (SFERA project, Solar Facilities for the European Research Area). The Cimel sun photometer at DLR was calibrated at AERONET-EUROPE, supported by the FP7-funded ACTRIS (Aerosols, Clouds, and Trace gases Research InfraStructure Network) project. The support provided by the AERONET, PHOTONS and RIMA staff with the sun photometer calibration and data evaluation is much appreciated.

References

Ångström, A., 1961. Radiation to actinometric receivers in its dependence on aperture conditions. Tellus 13, 425–431.

Ångström, A., Rohde, B., 1966. Pyrheliometric measurements with special regard to the circumsolar sky radiation. Tellus 18, 25–33. http://dx.doi.org/10.1111/j.2153-3490.1966.tb01440.x.

Batlles, F., Olmo, F., Alados-Arboledas, L., 1996. On shadowband correction methods for diffuse irradiance measurements. Sol. Energy 54, 105–114. http://dx.doi.org/10.1016/0038-092X(94)00115-T.

Belhomme, B., Pitz-Paal, R., Schwarzbözl, P., Ulmer, S., 2009. A new fast ray tracing tool for high-precision simulation of Heliostat fields. J. Sol. Energy Eng. 131, 031002.

Bendt, P., Rabl, A., 1981. Optical analysis of point focus parabolic radiation concentrators. Appl. Opt. 20 (4), 674–683.

Bendt, P., Rabl, A., Gaul, H.W., Reed, K.A., 1979. Optical Analysis and Optimization of Line Focus Solar Collectors. SERI/TR-34-092. Technical Report, National Renewable Energy Laboratory (NREL), Golden, CO. <http://citeseerx.ist.psu.edu/viewdoc/download?doi=10.1.1.129.5191&rep=rep1&type=pdf> (last accessed 05.12.14).

Benz, N., Kuckelkorn, Th., 2004. A new receiver for parabolic trough collectors fields. In: 12th SolarPACES Int. Symposium, Oxaca (Mexico).

Berk, A., Bernstein, L., Anderson, G., Acharya, P., Robertson, D., Chetwynd, J., Adler-Golden, 1998. MODTRAN cloud and multiple scattering upgrades with application to AVIRIS. Rem. Sens. Environ. 65 (3), 367–375.

Biggs, F., Vittitoe, C.N., 1977. Helios: A Computational Model for Solar Concentrators. OSTI ID: 5385022. Report Number(s): SAND-77-1185C; CONF-770850-1. DOE Contract Number: EY-76-C-04-0789. Sandia Labs. Resource Relation: Conference: ERDA Solar Workshop on Methods for Optical Analysis of Central Receiver Systems, Houston, TX, USA.

Blanc, P., Espinar, B., Wald, L., 2013. Report on Direct Normal Irradiance Standards. MACC-II, Technical Report D121.1.

Buck, R., 2010. Solar Power Raytracing Tool SPRAY User Manual. Technical Report.

Buie, D., Monger, A.G., 2004. The effect of circumsolar radiation on a solar concentrating system. Sol. Energy 76, 181–185. http://dx.doi.org/10.1016/j.solener.2003.07.032.

Buie, D., Dey, C.J., Bosi, S., 2003a. The effective size of the solar cone for solar concentrating systems. Sol. Energy 74, 417–427.

Buie, D., Monger, A.G., Dey, C., 2003b. Sunshape distributions for terrestrial solar simulations. Sol. Energy 74 (2), 113–122. http://dx.doi.org/10.1016/S0038-092X(03)00125-7.

Dersch, J., Schwarzbözl, P., Richert, T., 2011. Annual yield analysis of solar tower power plants with GREENIUS. J. Sol. Energy Eng. 133 (3), 031017. http://dx.doi.org/10.1115/1.4004355, 9 pp.

EKO Instruments Europe B.V., 2011. MS-56 DNI Sensor. Unprecedented Performance for Leading-Edge Research.

Finsterle, W., Fehlmann, A., Schmutz, W., 2012. The 11th international pyrheliometer comparison and a saharan dust event. In: Proc. WMO Technical Conference on Meteorological and Environmental Instruments and Methods of Observation, TECO-2012, Brussels, Belgium, 16–18 October 2012. <http://www.knmi.nl/samenw/geoss/wmo/TECO2012/> (last accessed 01.15.14).

Geuder, N., Quaschning, V., 2006. Soiling of irradiation sensors and methods for soiling correction. Sol. Energy 80 (11), 1402–1409.

Geuder, N., Trieb, F., Schillings, C., Meyer, R., Quaschning, V., 2003. Comparison of different methods for measuring solar irradiation data. In: 3rd International Conference on Experiences with Automatic Weather Stations.

Geuder, N., Pulvermueller, B., Vorbrugg, O., 2008. Corrections for rotating shadowband pyranometers for solar resource assessment, In: SPIE7046 Optical Modeling and Measurements for Solar Energy Systems II. doi:http://dx.doi.org/10.1117/12.797472.

Geuder, N., Hanussek, M., Haller, J., Affolter, R., Wilbert, S., 2011. Comparison of corrections and calibration procedures for rotating shadowband irradiance sensors. In: 17th Solar Paces International Symposium, Granada, Spain.

Gilman, P., Blair, N., Mehos, M., Christensen, C., Janzou, S., Cameron, C., 2008. Solar Advisor Model User Guide for Version 2.0. National Renewable Energy Laboratory, NREL/TP-670-43704, 133 pp.

Gnos, M., 2010. On the Development of a Low Cost Pyrheliometer. Graduate School Thesis, Florida State University, 128 pp. doi:http://dx.doi.org/10.1115/ES2010-90418.

Grether, D., Nelson, J., Wahlig, M., 1975. Measurement of Circumsolar Radiation. Progress Report. Technical Report NSF/RANN/SE/AG-536/PR/74/4.

Grether, D, Hunt, A., Wahlig, M., 1977. Circumsolar Radiation: Correlations with Solar Radiation. Lawrence Berkeley National Laboratory.

Gueymard, C.A., 1995. SMARTS, a Simple Model of the Atmospheric Radiative Transfer of Sunshine: Algorithms and Performance Assessment. Technical Report FSEC-PF-270-95, Florida Solar Energy Center, Cocoa, FL. <http://www.solarconsultingservices.com/SMARTS2_report.pdf> (last accessed 05.15.14).

Gueymard, C.A., 1998. Turbidity determination from broadband irradiance measurements: a detailed multi-coefficient approach. J. Appl. Meteorol. 37, 414–435.

Gueymard, C.A., 2001. Parameterized transmittance model for direct beam and circumsolar spectral irradiance. Sol. Energy 71 (5), 325–346.

Gueymard, C.A., 2005. SMARTS Code (Version 2.9.5). User's Manual, 50 pp. <http://rredc.nrel.gov/solar/models/SMARTS/relatedrefs/SMARTS295_Users_Manual_PC.pdf> (last accessed 01.15.14).

Gueymard, C.A., 2010. Spectral circumsolar radiation contribution to CPV. In: CPV-6 Conf., Freiburg, Germany; AIP Conf. Proc., vol. 1277, pp. 31.

Gueymard, C.A., 2010. Solar resource assessment for CSP and CPV, Pt. 2. In: Fifth session of the 2nd Concentrated Solar Power Training, Webinar 28 October 2010. <http://www.leonardo-energy.org> (last accessed 01.15.14).

Gueymard, C.A., Myers, D.R., 2008. Solar radiation measurement: progress in radiometry for improved modeling. In: Badescu, V. (Ed.), Modeling Solar Radiation at the Earth Surface. Springer.

Hess, M., Köpke, P., Schult, I., 1998. Optical properties of aerosols and clouds: the software package OPAC. Bull. Am. Meteorol. Soc. 79, 831–844.

Hukseflux, 2011. Product Specifications – DR02 Fast Response First Class Pyrheliometer with Heated Window.

IRENA, 2012. Concentrating Solar Power, International Renewable Energy Agency, Working Paper, Renewable Energy Technologies: Cost Analysis Series, vol. 1, Issue (2/5), 48 pp.

ISO 9488, 1999. Solar Energy: Vocabulary.

King, D.L., Boyson, W.E., Hansen, B.R., Bower, W.I., 1998. Improved low-cost solar irradiance sensors. In: 2nd World Conference and

Exhibition on Photovoltaic Solar Energy Conversion, 6–10 July, Vienna, Austria.
Kipp, Zonen, 2008. CHP1 Pyrheliometer Instruction Manual (Version 0811).
Kistler, B.L., 1986. A User's Manual for DELSOL3: A Computer Code for Calculating the Optical Performance and Optimal System Design for Solar Thermal Central Receiver Plants. Sandia National Labs, SAND86-8018, 239 pp.
Kocifaj, M., Gueymard, C.A., 2011. Theoretical evaluation of errors in aerosol optical depth retrievals from ground-based direct-sun measurements due to circumsolar and related effects. Atmos. Environ. 45, 1050–1058. http://dx.doi.org/10.1016/j.atmosenv.2010.07.054.
Leary, P.L., Hankins, J.D., 1979. User's Guide for MIRVAL: A Computer Code for Comparing Designs of Heliostat-receiver Optics for Central Receiver Solar Power Plants. Technical Report, SAND-77-8280, Sandia Labs., Livermore, CA (USA).
Lemperle, G., 1982. Effect of Sunshape on Flux Distribution and Intercept Factor of the Solar Tower Power Plant at Almería. SSPS No. 3/82. Technical Report, Deutsche Forschungs- und Versuchsanstalt für Luft-und Raumfahrt e.V., Köln (Germany).
Linke, F., 1931. Die Bedeutung des Öffnungsverhaltnisses eines Aktinometers für Messugen des Sonnen und Himmelstrahlung. Strähelentherapie 39, 351.
Linke, F., Ulmitz, E., 1940. Messungen der zirkumsolaren Himmelstrahlung. Met. Zeit. 57, 372–375.
Liou, K., 2002. An Introduction to Atmospheric Radiation, second ed. Academic Press.
López, G., Muneer, T., Claywell, R., 2004. Assessment of four shadow band correction models using beam normal irradiance data from the United Kingdom and Israel. Energy Convers. Manage. 45, 1963–1979. http://dx.doi.org/10.1016/j.enconman.2003.11.001.
Major, G., 1973. An effect of the circumsolar sky radiation on the Ångström Pyrheliometric scale. Tellus 25, 396–399.
Major, G., 1980. A method for determining the circumsolar sky function. Tellus 32, 340–347. http://dx.doi.org/10.1111/j.2153-3490.1980.tb00961.x.
Major, G., 1992. Estimation of the error caused by the circumsolar radiation when measuring global radiation as a sum of direct and diffuse radiation. Sol. Energy 48 (4), 249–252.
Major, G., 1994. Circumsolar Correction for Pyrheliometers and Diffusometers. WMO Report 635.
Mayer, B., 2009. Radiative transfer in the cloudy atmosphere. Eur. Phys. J. Conf. 1, 75–99. http://dx.doi.org/10.1140/epjconf/e2009-00912-1.
Mayer, B., Kylling, A., 2005. Technical note: the libRadtran software package for radiative transfer calculations – description and examples of use. Atmos. Chem. Phys. Discuss. 5 (2), 1319–1381.
Meyen, S., Lüpfert, E., 2009. Measurement of Reflectivity of Optical Components for Concentrating Solar Power Technology, DLR, Test Report, 14 pp.
Michalsky, J.J., Berndt, J.L., Schuster, G.J., 1986. A microprocessor-controlled rotating shadowband radiometer. Sol. Energy 36, 465–470.
Middleton Solar, 2008. DN5 and DN5-E First Class Pyrheliometer User's Guide.
Mishchenko, M.I., 2011. Directional radiometry and radiative transfer: a new paradigm. J. Quant. Spectros. Rad. Transf. 112, 2079–2094.
Mishchenko, M.I., 2014. Directional radiometry and radiative transfer: the convoluted path from centuries-old phenomenology to physical optics. J. Quant. Spectros. Rad. Transf. 146, 4–33.
Neumann, A., Von Der Au, B., 1997. Sunshape measurements at the DLR solar furnace site in Cologne, Germany. Int. Solar Energy Conf.. American Society of Mechanical Engineers, Washington, DC, pp. 163–170.
Neumann, A., Witzke, A., 1999. The influence of sunshape on the DLR solar furnace beam. Sol. Energy 66 (6), 447–457.
Neumann, A., Witzke, A., Jones, S.A., Schmitt, G., 2002. Representative terrestrial solar brightness profiles. J. Sol. Energy Eng. 124, 198–204.
Noring, J.E., Grether, D.F., Hunt, A.J., 1991. Circumsolar Radiation Data: The Lawrence Berkeley Laboratory Reduced Data Base. Technical Report, NREL/TP-262-4429, National Renewable Energy Lab., Golden, CO (United States); Lawrence Berkeley Lab., CA (United States).
Pape, B., Batlles, J., Geuder, N., Zurita Piñero, R., Adan, F., Pulvermueller, B., 2009. Soiling impact and correction formulas in solar measurements for CSP projects. In: 15th Solar Paces International Symposium, Berlin, Germany.
Pastiels, R., 1959. Contribution à l'étude du problème des méthodes actinométriques. Institut Royal Météorologique de Belgique, Publ. A11.
Pierce, A.K., Slaughter, C.D., 1977. Solar limb darkening I: λλ (3033–7297). Sol. Phys. 51, 25–41.
Quaschning, V., Ortmanns, W., Kistner, R., Geyer, M., 2001. Greenius: a new simulation environment for technical and economical analysis of renewable independent power projects. In: Solar Forum 2001 – Solar Energy: The Power to Choose, Washington, DC, U.S.
Rabl, A., 1976. Comparison of solar concentrators. Sol. Energy 18, 93–111.
Rabl, A., 1985. Active Solar Collectors and their Applications. Oxford U. Press, New York, 503 pp., ISBN 0195035461.
Rabl, A., Bendt, P., 1982. Effect of circumsolar radiation on performance of focussing collectors. J. Sol. Energy Eng. 104 (3), 237–250. http://dx.doi.org/10.1115/1.3266308.
Reinhardt, B., 2013. On the Retrieval of Circumsolar Radiation from Satellite Observations and Weather Model Output. Dissertation, LMU München. <http://nbn-resolving.de/urn:nbn:de:bvb:19-164380> (last accessed 05.12.14).
Reinhardt, B., Buras, R., Bugliaro, L., Wilbert, S., Mayer, B., 2014. Determination of circumsolar radiation from Meteosat Second Generation. Atmos. Meas. Tech. 7, 823–838. http://dx.doi.org/10.5194/amt-7-823-2014.
Rüedi, I., 2000. Results and Symposium, International Pyrheliometer Comparison, IPC-IX, 25 September–13 October, Davos, Switzerland, doi: http://dx.doi.org/10.3929/ethz-a-004371547.
Rüedi, I., Finsterle, W., 2005. The World Radiometric Reference and its quality system. In: Proc. WMO Tech. Conf. on Meteorological and Environmental Instruments and Methods of Observation (TECO-2005), Instruments and Observing Methods, Bucharest, Romania, Government of Romania, Rep. 82, WMO/TD 1265, pp. 434–436. <https://www.wmo.int/pages/prog/www/IMOP/publications/IOM-82-TECO_2005/Papers/3(15)_Switzerland_Ruedi.pdf> (last accessed 05.12.14).
Schubnell, M., 1992. Influence of circumsolar radiation on aperture, operating temperature and efficiency of a solar cavity receiver. Sol. Energy Mater. Sol. Cells 27 (3), 233–242.
Schwarzbözl, P., 2009. The User's Guide to HFLCAL. A Software Program for Heliostat Field Layout Calculation. Software Release Visual HFLCAL VH12. DLR.
Vignola, F., 2006. Removing systematic errors from rotating shadowband pyranometer data. In: Proc. of the 35th ASES Annual Conference, Denver, CO, 6 pp.
Vignola, F., Michalsky, J., Stoffel, T., 2012. Solar and Infrared Radiation Measurements (Energy and the Environment). CRC Press, Taylor & Francis Group, 402 pp., ISBN 978-1-4398-5189-0.
Vittitoe, C., Biggs, F., 1981. User's Guide to HELIOS: A Computer Program for Modeling the Optical Behavior of Reflecting Solar Concentrators (Part 1). Sandia National Labs, SAND 91-1180.
Wendelin, T., 2003. SolTRACE: a new optical modeling tool for concentrating solar optics. In: ISEC2003-44090, pp. 253–260.
Wilbert, S., 2014. Determination of Circumsolar Radiation and its Effect on Concentrating Solar Power. PhD Thesis, Rheinisch-Westfälische Technische Hochschule Aachen, DLR.
Wilbert, S., Pitz-Paal, R., Müller, S., 2012. Rotating shadowband irradiometers and circumsolar radiation. In: COST WIRE Workshop, Payerne, Switzerland.
Wilbert, S., Reinhardt, B., DeVore, J., Roeger, M., Pitz-Paal, R., Gueymard, C.A., Buras, R., 2013a. Measurement of solar radiance profiles with the sun and aureole measurement system. J. Sol. Energy Eng. 135, 1–11. http://dx.doi.org/10.1115/1.4024244.

Wilbert, S., Pitz-Paal, R., Jaus, J., 2013b. Comparison of measurement techniques for the determination of circumsolar irradiance. In: Proc. of the International Conference on Concentrator Photovoltaic Systems (CPV-9), Miyasaki, Japan.

Wilbert, S., Geuder, N., Lüpfert, E., Pottler, K., Pitz-Paal, R., 2013c. Sunshape measurements with rotating shadowband irradiometers (RSI). In: DLR CSPS. <http://www.cspservices.eu/files/downloads/CSPS_DLR_RSI-sunshape_1309m.pdf> (last accessed 05.12.14).

Willson, R.C., 1969. Experimental and Theoretical Comparison of the International Pyrheliometric Scale, Technical Report 32-7365, NASA, 32 pp.

WMO, 1967. Précisions des mesures pyrhéliométriques, Tech. note No. 85. <http://library.wmo.int/opac/index.php?lvl=notice_display&id=5578> (last accessed 05.12.14).

WMO, 2010. CIMO guide to meteorological instruments and methods of observation . In: Measurement of Radiation, World Meteorological Organization, WMO-No. 8 (2010 update), seventh ed. Geneva, Switzerland, pp. 157–198 (Chapter 7).

Wolfertstetter, F., Pottler, K., Merrouni, A.A., Mezrhab, A., Pitz-Paal, R., 2012. A novel method for automatic real-time monitoring of mirror soiling rates. In: 18th Solar Paces International Symposium, Marrakesh, Morocco.

Wolfertstetter, F., Pottler, K., Geuder, N., Affolter, R., Merrouni, A.A., Mezrhab, A., Pitz-Paal, R., 2013. Monitoring of mirror and sensor soiling with TraCS for improved quality of ground based irradiance measurements. In: 19th Solar Paces International Symposium, Las Vegas, USA.

Wood, J.G., 1999. Solar Radiation Sensor. Patent WO 99/13359.

Zdunkowski, W., Trautmann, T., Bott, A., 2007. Radiation in the Atmosphere: A Course in Theoretical Meteorology. Cambridge University Press, ISBN 978-0-521-87107-5.